THE EFFECTS OF SWELLS ON TURBULENCE STRUCTURE OVER WAVY WALLS

Takanori Imashiro
Department of Mechanical Engineering and Science, Kyoto University
Yoshida-honmachi, Sakyo-ku, Kyoto 606-8501, Japan
takanori@t01.mbox.media.kyoto-u.ac.jp

Toshiyuki Yamamoto
Department of Mechanical Engineering and Science, Kyoto University
Yoshida-honmachi, Sakyo-ku, Kyoto 606-8501, Japan
yamamoto-toshiyuki@t05.mbox.media.kyoto-u.ac.jp

Ryoichi Kurose
Department of Mechanical Engineering and Science and Advanced Research Institute of Fluid Science and Engineering, Kyoto University
Yoshida-honmachi, Sakyo-ku, Kyoto 606-8501, Japan
kurose@mech.kyoto-u.ac.jp

Satoru Komori
Department of Mechanical Engineering and Science and Advanced Research Institute of Fluid Science and Engineering, Kyoto University
Yoshida-honmachi, Sakyo-ku, Kyoto 606-8501, Japan
komori@mech.kyoto-u.ac.jp

ABSTRACT

Three-dimensional direct numerical simulations (DNS) are applied to turbulent boundary layers over the wavy walls, which imitate air-water interfaces with pure wind-wave and swells, and the effects of parallel and oblique swells on the turbulence structure and drag forces are investigated. The results show that both parallel and oblique swells increase the turbulence intensities and the Reynolds stress over the wavy walls. The swells also increase the pressure drag and decrease the friction drag on the wavy walls, and consequently increase total drag because of the remarkable increase of the pressure drag. These effects are smaller for the oblique swell than that for the parallel swell. This suggests that the swells suppress the mass transfer across the air-water interface, but the effect becomes weak by their obliqueness.

INTRODUCTION

Global warming, which has become one of the most serious environmental problems in recent decades, is thought to be caused by emissions of green house gasses such as carbon dioxide (CO_2) and methane (CH_4). In order to predict the increase in the atmospheric temperature, therefore, it is of great importance to precisely estimate the mass transfer rate across the air-sea interface between atmosphere and oceans for such gases.

In GCM (General Circulation Model) climate simulations, the mass transfer rate has been correlated with only wind speed observed over oceans (Wanninkhof *et al.*, 1992). However, the relation between the mass transfer rate and the wind velocity is much scattered. One of the reasons why the field measurements are so scattered is considered to be that there exist some other factors affecting the air-sea mass transfer. Generally, there exist two types of wave in oceans, namely, pure wind-wave generated by only wind shear on the air-water interface and swell propagated from faraway with low frequency. In our previous experiments using a wind-wave tank (Tanno *et al.*, 2004), it was found that swell decreases the mass transfer rate across the air-water interface with wind-wave. However, it has not been clarified why the swell reduces the mass transfer rate. To clarify the swell effect, fluid forces acting on the interface should be carefully investigated, since the mass transfer rate is strongly affected by surface-renewal eddies beneath the air-sea interface, which are produced mainly by the fluid forces on the interface.

Three-dimensional direct numerical simulation (DNS) of air-water two phase flows may be one of the useful tools for investigating the turbulence structure in both air and water flows and the fluid forces on the interface. However, the DNS will require huge computation time especially for the interface with wind-wave and swells. To save the computation time and to qualitatively discuss the swell effects, it is practical to apply the DNS to only air flow over wavy rigid walls with similar shapes to the interfaces with wind-wave and swells.

The turbulent flow over wavy rigid walls has been examined in many studies. For example, Zilker *et al.* (1977) investigated the influence of the amplitude of wavy wall by experiment. Komori (1996) investigated the turbulence structure over three-dimensional wavy wall by DNS. Ange-

Table 1: Shapes of wavy walls.

Case	Function	Wave type	θ
1	$0.055/2\lambda\cos(2\pi\cdot x/\lambda)$	pure wind-wave	—
2	$0.055/2\lambda\cos(2\pi\cdot x/\lambda)$ $+0.225/2\lambda\cos(\pi/2\cdot x/\lambda)$	wind-wave with parallel swell	0°
3	$0.055/2\lambda\cos(2\pi\cdot x/\lambda)$ $+0.225/2\lambda\cos(\pi/6\cdot(2x+\sqrt{5}y)/\lambda)$	wind-wave with oblique swell	48°

lis *et al.* (1997) investigated the effect of wall's wavelength by DNS. Nakagawa *et al.* (2001) measured the turbulence structure using PIV (Particle Image Velocimetry). Recently, Nakayama *et al.* (2003) investigated the turbulence flow over the complex wavy wall which had two waves of different wavelength. However, the drag forces on the wavy walls have not been investigated well.

The purpose of this study is, therefore, to clarify the swell effects on turbulence structure and fluid forces on the interfaces by applying three-dimensional DNS to turbulent air flows over wavy walls, which imitate air-water interfaces with wind-wave and swells. Three types of walls, pure wind-wave, wind-wave with parallel swell, and wind-wave with oblique swell, are considered in this study.

DIRECT NUMERICAL SIMULATION

The continuity equation and three-dimensional Navier-Stokes equations for incompressible fluids;

$$\frac{\partial U_i}{\partial x_i} = 0, \tag{1}$$

$$\frac{\partial U_i}{\partial t} + U_j\frac{\partial U_i}{\partial x_j} = -\frac{1}{\rho}\frac{\partial P}{\partial x_i} + \nu\frac{\partial^2 U_i}{\partial x_j \partial x_j}, \tag{2}$$

were directly solved using the finite difference method (Marker and Cell method). The details of the numerical method and accuracy of the present DNS are described in our previous study (Komori *et al.*, 1993). Turbulent air flows over three wavy walls; pure wind-wave (case 1), wind-wave with parallel swell (case 2) and wind-wave with oblique swell (case 3), were computed. The computational domains for cases $1\sim3$ are shown in Fig. 1. The computational domains for cases 1 and 2 were $8\lambda\times4\lambda\times5.2\lambda$ in the x, y and z directions and the numbers of grid points were $200\times100\times200$. The computational domain for case 3 was $12\lambda\times\frac{12\sqrt{5}}{5}\lambda\times5.2\lambda$ and the number of grid points was $300\times134\times200$. Here, λ ($=1.0\times10^{-2}$m) is the wavelength of the wind-wave.

The wind-wave and swells were approximated as sinusoidal waves and the shapes of wind-wave with swells were acquired as the sum of their sinusoidal functions. The wave heights of the wind-wave and the swells were 0.055λ and 0.225λ and the wavelengths of them were λ and 4λ, respectively. In case 3, the inclination angle of swell, θ, is $\tanh(\frac{\sqrt{5}}{2}) \simeq 48^\circ$, which was defined to satisfy both the streamwise and spanwise periodic conditions. The shapes of the wavy walls are summarized in table 1. Periodic boundary conditions were applied in the streamwise and spanwise directions. Non-slip boundary conditions were applied on both the upper flat wall and the lower wavy wall. The wind was driven in the x direction over the wavy wall by the constant mean pressure gradient, which was equivalent in all cases. The Reynolds number, $Re = \frac{U_{max}\cdot H}{\nu}$, defined by maximum streamwise velocity, U_{max}, half height of the computational domain, $H(=2.6\lambda)$, and kinematic viscosity,ν, were 9,800 $\sim$ 11,800.

RESULTS AND DISCUSSION

TURBULENCE STRUCTURE OVER WAVY WALLS

Fig. 2 shows the distributions of instantaneous streamwise velocity on the $x-z$ plane. Turbulent flows are observed to be developed over the wavy walls in all cases. In cases 2 and 3, the streamwise velocity indicates negative value on the leeward side of the swells. This is because the reverse flow is generated by separated flow on this side. The reverse flow is stronger in case 2 than that in case 3.

Fig. 3 shows the distribution of instantaneous spanwise velocity on the $y-z$ plane in case 3. The spanwise velocity indicates remarkable negative value on the windward side of the oblique swell (Ⓐ). This is because the oblique swell guides the flow near the wavy wall. This result consists with fig. 4 which shows the instantaneous velocity vectors near the wavy wall in case 3. The velocity indicates negative spanwise value on the windward side of the oblique swell and weakly positive value on the top of it.

Fig. 5 shows the distribution of mean velocities in case 3. These values were obtained by time- and space-averaging in the streamwise and spanwise directions in the region over the top of wavy walls. (Other turbulence statistics were also calculated in the same way.) Mean streamwise velocity is small near the upper and lower walls as in general channel flows. It is also found that the velocity near the lower wavy wall is smaller than that near the upper flat wall. Additionally, the location where the velocity indicates the maximum value is higher than the center of domain. These are because the drag force on the lower wavy walls is larger than that on the upper flat wall, as mentioned later. The vertical velocity is zero in whole region, but the spanwise velocity indicates negative value. This consists with Figs. 3 and 4.

Fig. 6 shows the distributions of mean streamwise velocity in all cases. These values are non-dimensionalized by friction velocity, u_*, calculated from total drag force on the wavy walls, $D_{T,w}$, which is mentioned later. The distributions have the log-law region in all cases. Since the forced pressure gradient is same but the drag forces on the wavy walls are different, their maximum velocities are different.

Figs. 7 and 8 show the distributions of turbulent intensities and the Reynolds stress, respectively. These values are non-dimensionalized by u_* and shown only for wavy wall side. The turbulent intensities and the Reynolds stress in cases 2 and 3 are found to be stronger than those in case 1. This indicates that both the parallel and oblique swells promote turbulence over the wind-driven air-water interface.

DRAG FORCES ON WAVY WALLS

Pressure drag, D_P, and friction drag, D_F, were calculated by integrating pressure and shear stress on the wavy walls, respectively, as

$$D_P = -\frac{1}{A}\int\int_S p_w \boldsymbol{e_n}\cdot\boldsymbol{e_x}\, dS, \tag{3}$$

$$D_F = \frac{1}{A}\int\int_S \tau_w \boldsymbol{e_l}\cdot\boldsymbol{e_x}\, dS, \tag{4}$$

where p_w and τ_w denote the local mean pressure and local mean streamwise shear stress, respectively. $\boldsymbol{e_n}$, $\boldsymbol{e_l}$ and $\boldsymbol{e_x}$

are wall normal vector, wall tangential vector and streamwise unit vector, respectively, and A denotes vertical projected area of the walls. Since the flows in this study are a kind of channel flow, there is a friction drag force on the flat wall, $D_{F,f}$, in addition to pressure drag force and friction drag force on the wavy walls, $D_{P,w}$ and $D_{F,w}$. Their ratios to the total drag force, $D_T(= D_{F,f} + D_{P,w} + D_{F,w})$, are shown in Fig. 9. It is found that the parallel and oblique swells reduce the friction drag and promote the pressure drag acting on the wavy walls. The total drag on wavy walls, $D_{T,w}(= D_{P,w} + D_{F,w})$, is increased by the swells because of the rapid increase of pressure drag. However, the effect is smaller for the oblique swell than that for the parallel swell. The fact that the friction drag generates surface renewal eddies beneath the real air-water interface suggests that the decrease of friction drag by the swells results in the reduction of mass transfer rate across the wind-driven air-water interface and that the reduction effect is weakened by the obliqueness of swell. Therefore, not only wind but also swell should be taken into account in estimating the mass transfer rate.

SHEAR STRESS AND PRESSURE DISTRIBUTIONS ON WAVY WALLS

In order to elucidate the reason why pressure drag is increased and friction drag is reduced by swells, local pressure and shear stress on the wavy walls were examined. Figs. 10 and 11 show the streamwise distributions of the mean pressure on the wavy walls. In these figures, the shapes of wavy walls in cases 2 and 3 are also illustrated. It is found that the pressure is high at the trough of wind-wave and low at the crest of them in all cases. Also the pressure is higher for the wind-wave with swell (cases 2 and 3) than that for the pure wind-wave (case 1) at the trough of swell, especially at the leeward side of trough. This is because the wavy wall blocks the stream at the leeward side of trough. However, the increasing rate of pressure by the oblique swell is smaller than that by the parallel swell, since the shape of wavy wall in the streamwise direction is blunter for the oblique swell (case 3) than that for the parallel swell (case 2). These results explain the swell effects on the pressure drag shown in Fig. 9.

Figs. 12 and 13 show the streamwise distributions of the mean streamwise shear stress on the wavy walls. It is observed that the streamwise shear stress is high at the windward side of wind-wave's crest and low at the leeward side of them in all cases. The streamwise shear stress is higher for the wind-wave with swell (cases 2 and 3) than that for the pure wind-wave (case 1) at the windward side of the swell crest, but lower at the leeward side of the swell crest. The effects of the oblique swell on the streamwise shear stress are weaker than those of parallel swell because of the bluntness of the oblique swell, as mentioned above. Comparing the amount of the decrease and that of the increase by swells, the former effect is bigger than the latter. These are consistent with the swell effects on the friction drag shown in Fig. 9.

CONCLUSIONS

Three-dimensional direct numerical simulations (DNS) were applied to turbulent boundary layers over the wavy walls, which imitate air-water interfaces with wind-wave and swells, and the effects of parallel and oblique swells on the turbulence structure and drag forces were investigated. The results are summarized as follows.

(1) The swells increase the turbulence intensities and the Reynolds stress over the wavy wall.
(2) The swells increase the pressure drag and decrease the friction drag on the wavy wall, and consequently increase total drag because of the remarkable increase of the pressure drag. These effects are smaller for the oblique swell than that for the parallel swell.
(3) It is suggested that the swells suppress the mass transfer across the air-water interface, but the effect becomes weak by the obliqueness of swells.

ACKNOWLEDGMENTS

This research was supported by the Ministry of Education, Science, Sports and Culture, Grant-in-Aid (No.14102016) and 21st Century Center of Excellence Program for Research and Education on Complex Functional Mechanical Systems. This simulation was performed by super computer of National Institute for Environmental Studies, Center for Global Environmental Research.

REFERENCES

Angelis, V. D., P. Lombardi & S. Banerjee, Direct numerical simulation of turbulent flow over a wavy wall, *Phys. Fluids A*, **9** (1997), 2429-2442.

Zilker, D. P., G. W. Cook & T. J. Hanratty, Influence of the amplitude of a solid wavy wall on a turbulent flow. Part1. Non-separated flows, *J. Fluid Mech.*, **82** (1977), 29-51.

Komori, S., Turbulence structure and CO_2 transfer at the air-sea interface and turbulent diffusion in thermally-stratified flows, *CGER's Supercompute Monograph Report*, **1**, Centre for Global Environmental Research, National Institute for Envionmental Studies, Environment Agency of Japan (1996).

Komori, S., R. Nagaosa, Y. Murakami, s. Chiba, K. Ishii & K. Kuwahara, Direct numerical simulation of three-dimensional open-channel flow with zero-shear gas-liquid interface, *Phys. Fluids A*, **5** (1993), 115-125.

Nakagawa, S. & T. J. Hanratty, Particle image velocimetry measurements of flow over a wavy wall, *Phys. Fluids A*, **13** (2001), 3504-3507.

Nakayama, A. & K. Sakio, Direct numerical simulation of turbulent flow over complex wavy rough surface, Journal of Applied Mechanics, JSCE **6** (2003), 839–846 (in Japanese).

Tanno, K., Komori, S., Effects of swell on turbulence structure and mass transfer across the wind-driven air-water interface, Trans. JSME. Ser. B., **70**-691 (2004), 644-649 (in Japanese).

Wanninkhof, R., Relationship between wind speed and gas exchange over the ocean, *J. Geophys. Res.*, **97** (1992), 7373–7382.

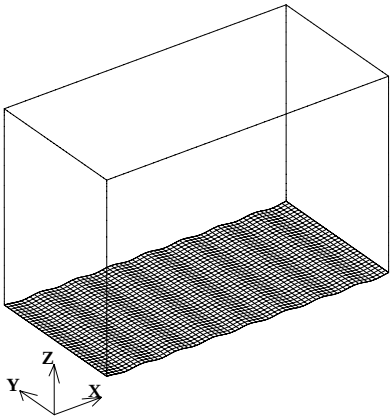

(a) Case 1 : Pure wind-wave.

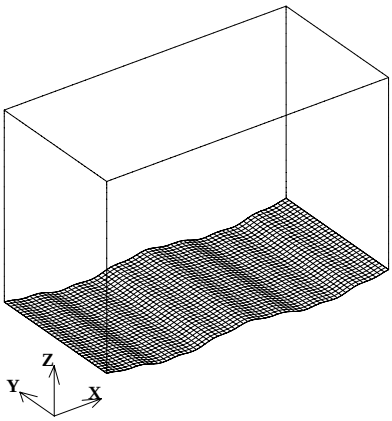

(b) Case 2 : Wind-wave with parallel swell.

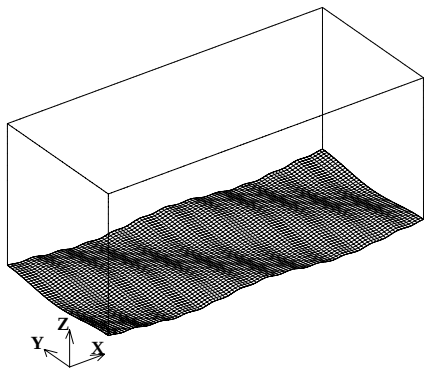

(c) Case 3 : Wind-wave with oblique swell.

Figure 1: Computational domains.

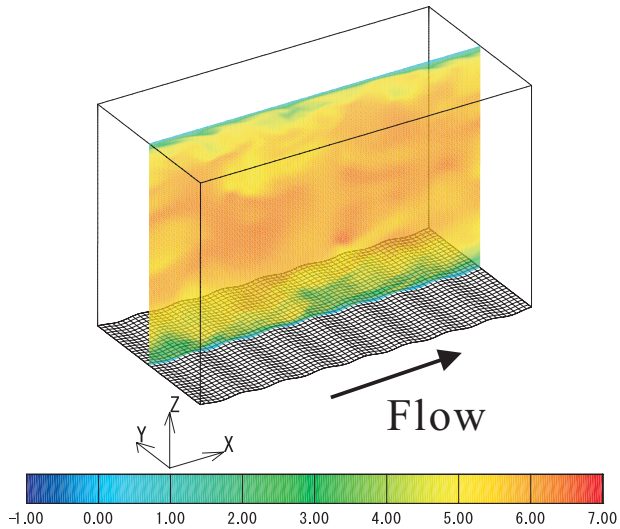

(a) Case 1 : Pure wind-wave.

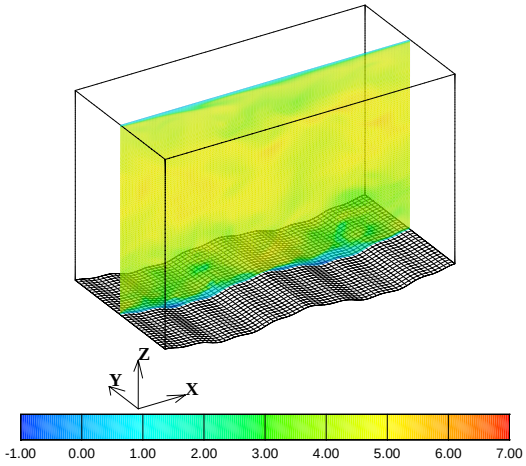

(b) Case 2 : Wind-wave with parallel swell.

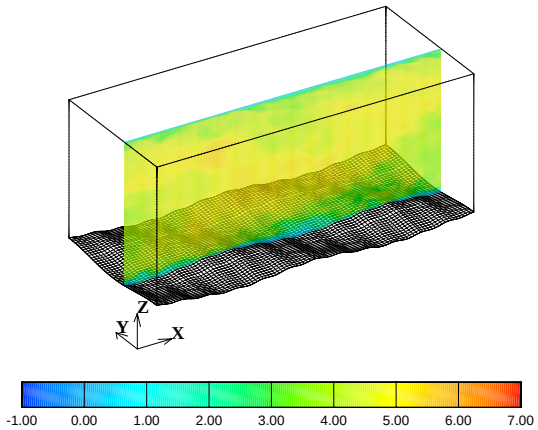

(c) Case 3 : Wind-wave with oblique swell.

Figure 2: Distributions of instantaneous streamwise velocity.

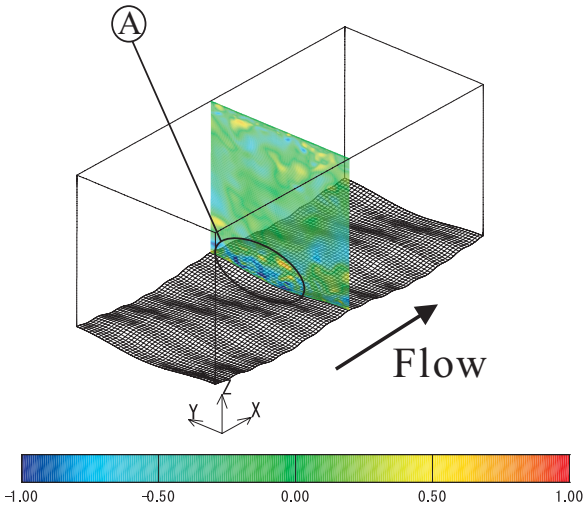

Figure 3: Distributions of instantaneous spanwise velocity in case 3.

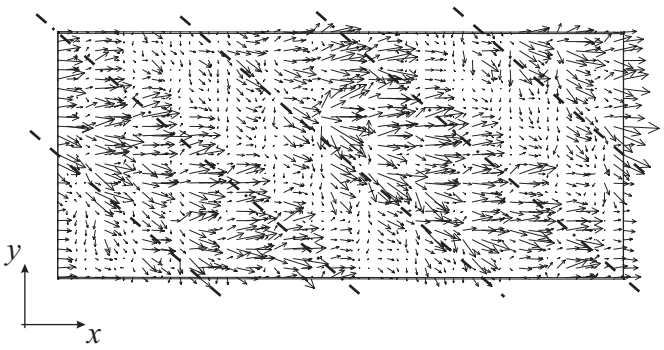

Figure 4: Instantaneous velocity vectors near the wavy wall in case 3. A dotted line -·-·- denotes the top of swell and dashed line - - - denotes the bottom of swell.

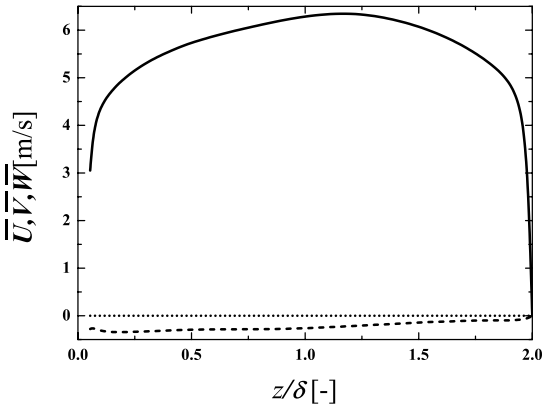

Figure 5: Distributions of mean velocities in case 3; ——, $\overline{U}$; - - - -, $\overline{V}$; ·····, $\overline{W}$.

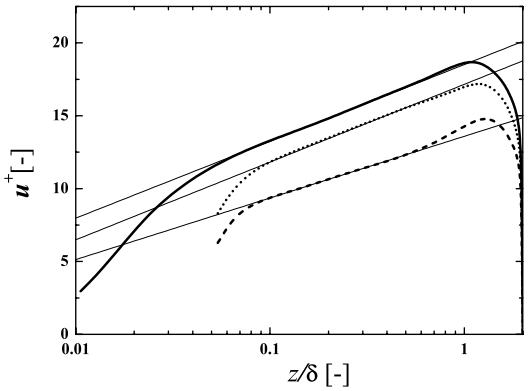

Figure 6: Distributions of mean streamwise velocity : ——, pure wind-wave (case 1); - - - -, wind-wave with parallel swell (case 2); ·····, wind-wave with oblique swell (case 3).

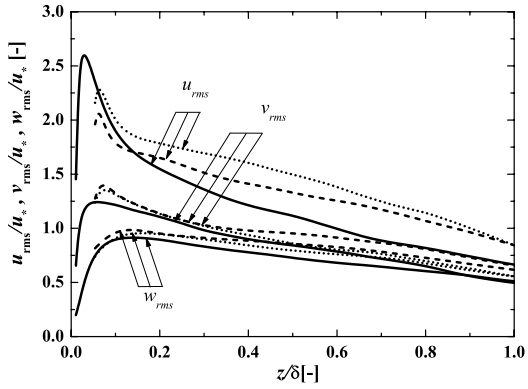

Figure 7: Distributions of turbulence intensities. Lines as in Fig. 6

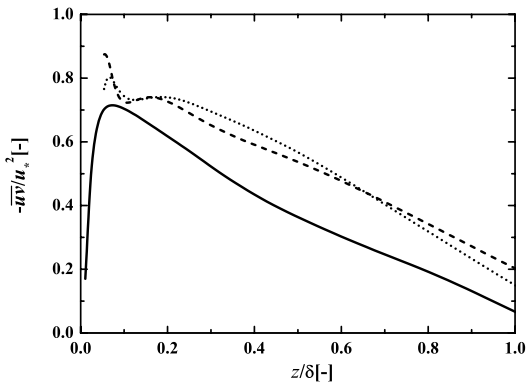

Figure 8: Distributions of the Reynolds stress. Lines as in Fig. 6

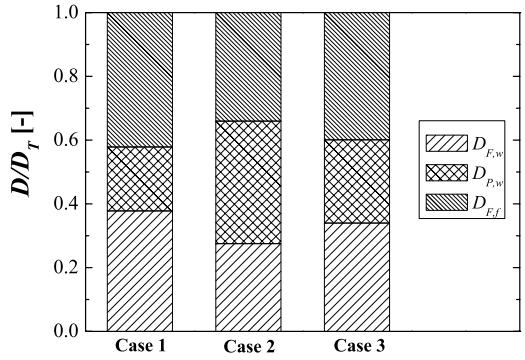

Figure 9: Drag forces acting on the top flat and bottom wavy walls.

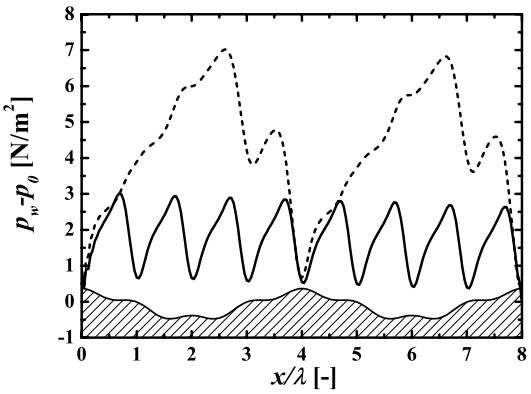

Figure 10: Distributions of pressure on the wavy walls : ——, pure wind-wave (case 1); - - - -, wind-wave with parallel swell (case 2).

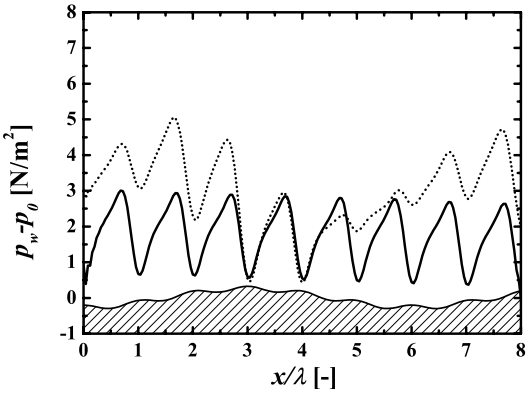

Figure 11: Distributions of pressure on the wavy walls. : ——, pure wind-wave (case 1); ·····, wind-wave with oblique swell (case 3).

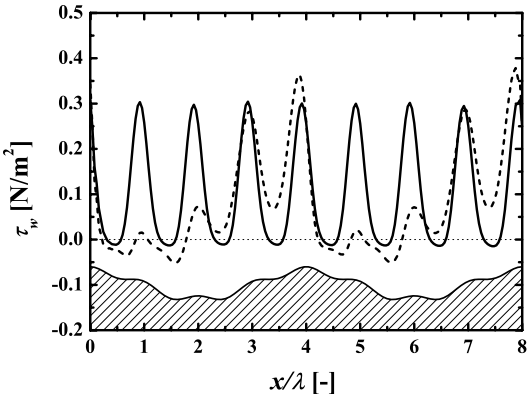

Figure 12: Distributions of shear stress on the wavy walls : ——, case 1; - - - -, case 2.

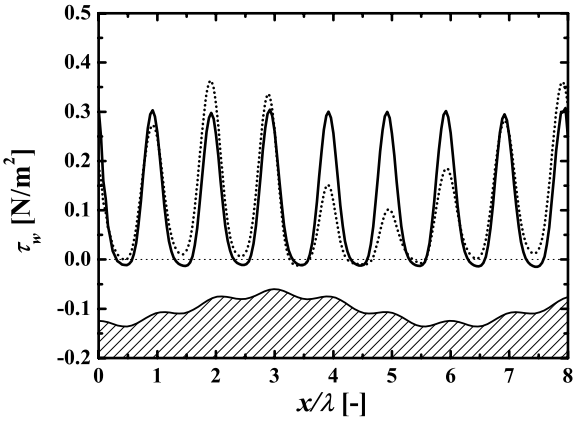

Figure 13: Distributions of shear stress on the wavy walls : ——, case 1; ·····, case 3 .